

Journal Pre-proof

Bis(diphenylamino)-Benzo[4,5]thieno[3,2-*b*]benzofuran as hole transport material for highly efficient RGB organic light-emitting diodes with low efficiency roll-off and long lifetime

Ming Shi, Yaowu He, Yue Sun, Daqi Fang, Jingsheng Miao, Muhammad Umair Ali, Tao Wang, Yunrui Wang, Tian Zhang, Hong Meng

PII: S1566-1199(20)30179-8

DOI: <https://doi.org/10.1016/j.orgel.2020.105793>

Reference: ORGELE 105793

To appear in: *Organic Electronics*

Received Date: 6 April 2020

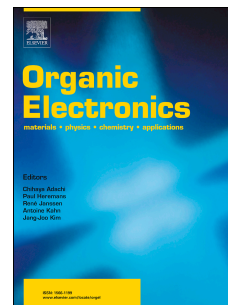
Revised Date: 25 April 2020

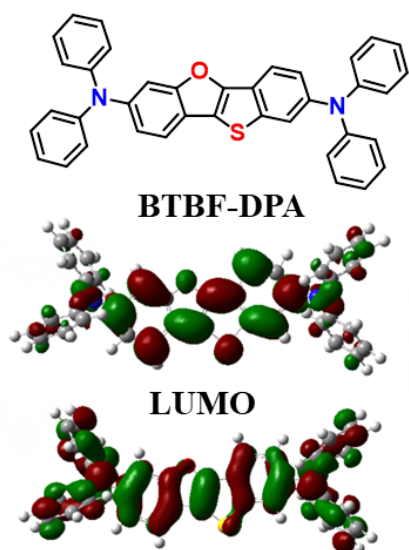
Accepted Date: 25 April 2020

Please cite this article as: M. Shi, Y. He, Y. Sun, D. Fang, J. Miao, M.U. Ali, T. Wang, Y. Wang, T. Zhang, H. Meng, Bis(diphenylamino)-Benzo[4,5]thieno[3,2-*b*]benzofuran as hole transport material for highly efficient RGB organic light-emitting diodes with low efficiency roll-off and long lifetime, *Organic Electronics* (2020), doi: <https://doi.org/10.1016/j.orgel.2020.105793>.

This is a PDF file of an article that has undergone enhancements after acceptance, such as the addition of a cover page and metadata, and formatting for readability, but it is not yet the definitive version of record. This version will undergo additional copyediting, typesetting and review before it is published in its final form, but we are providing this version to give early visibility of the article. Please note that, during the production process, errors may be discovered which could affect the content, and all legal disclaimers that apply to the journal pertain.

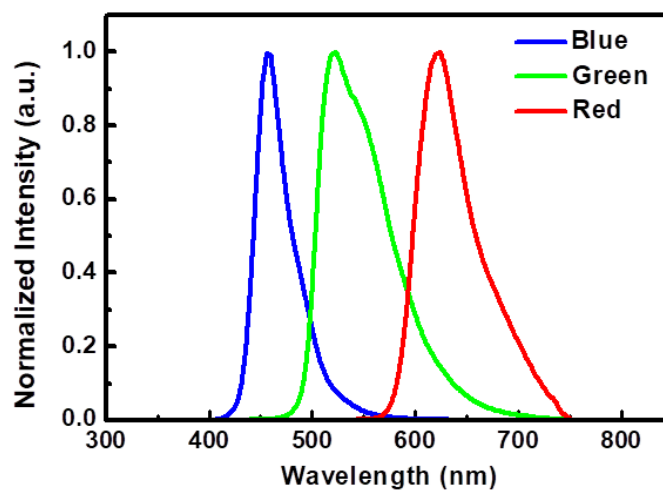
© 2020 Published by Elsevier B.V.





$$E_T = 2.99 \text{ eV}$$

$$\mu_h = 3.1 \times 10^{-5} \text{ cm}^2 \text{ V}^{-1} \text{ s}^{-1}$$



$$T_{99} = 70 \text{ h @ } 10000 \text{ cd m}^{-2} \quad \text{PE} = 40.1 \text{ lm W}^{-1}$$

$$T_{70} = 60 \text{ h @ } 10000 \text{ cd m}^{-2} \quad \text{PE} = 136.6 \text{ lm W}^{-1}$$

$$T_{80} = 125 \text{ h @ } 5000 \text{ cd m}^{-2} \quad \text{PE} = 4.9 \text{ lm W}^{-1}$$

Bis(diphenylamino)-Benzo[4,5]thieno[3,2-*b*]benzofuran as Hole Transport Material for Highly Efficient RGB Organic Light-Emitting Diodes with Low Efficiency Roll-off and Long Lifetime

*Ming Shi, Yaowu He, Yue Sun, Daqi Fang, Jingsheng Miao, Muhammad Umair Ali, Tao Wang, Yunrui Wang, Tian Zhang, Hong Meng**

School of Advanced Materials, Peking University Shenzhen Graduate School, Shenzhen, Shenzhen, 518055, P. R. China. E-mail: menghong@pku.edu.cn

KEYWORDS: BTBF, hole transport material, RGB OLEDs, power efficiency, lifetime

ABSTRACT: In this work, a novel hole transport material (HTM) based on benzo[4,5]thieno[3,2-*b*]benzofuran (BTBF) core with diphenylamine group, BTBF-DPA, was synthesized and systematically studied. BTBF-DPA showed high carrier mobility, good thermal stability and high triplet energy as 2.99 eV. Green phosphorescent organic light-emitting diodes (PhOLEDs) using BTBF-DPA were fabricated which displayed outstanding electroluminescent performance with a low turn-on voltage of 2.4 V, the maximum current efficiency (CE) of 123.6 cd A⁻¹, power efficiency (PE) of 136.6 lm W⁻¹, and external quantum efficiency (EQE) of 34.1%. Red PhOLEDs with BTBF-DPA also demonstrated a maximum PE of 40.1 lm W⁻¹, and EQE of 24.9% with a low turn-on voltage of 2.3 V. Besides, blue fluorescence OLEDs presented a maximum PE of 4.9 lm W⁻¹, EQE of 5.2% and small efficiency roll-off of 11.5% at 10000 cd

m^{-2} . RGB-OLEDs with BTBF-DPA outperformed the reference devices based on NPB as HTM that has been widely utilized. What's more, life-time of RGB OLEDs were $T_{99} = 70$ h at 10000 cd m^{-2} , $T_{70} = 60$ h at 10000 cd m^{-2} , $T_{80} = 125$ h at 5000 cd m^{-2} , respectively. These results imply that BTBF-DPA is a promising HTM for OLEDs.

1. INTRODUCTION

Organic light-emitting diodes (OLEDs) have attained great attention owing to their numerous applications as solid-state light emitting and flexible displays¹⁻⁴. There are several kinds of OLEDs according to the light-emitting mechanism, for example, phosphorescent or normal fluorescent system, thermal activated delayed fluorescent (TADF) system, triplet-triplet annihilation (TTA) system, hybridized local and charge-transfer excited state (HLCT) system, exciplex system and so on⁵⁻⁹. Many researches have been developed to optimize the emission layer to achieve as high as the EQE theoretical maximum¹⁰⁻¹³. While for commercial applications, the power efficiency (PE) of OLEDs is a crucial factor as it provides a direct measurement of the power consumption considering operating voltage and device life-time¹⁴⁻¹⁵. Typically, the efficiency of OLEDs will decrease with the increasing of brightness, which is efficiency roll-off. The efficiency roll-off reflects great influence on PE due to additional resistive losses¹⁶. In order to obtain high PE values at high brightness levels ($> 1000 \text{ cd m}^{-2}$), high current densities must be achieved at low voltage. This can be realized by using proper charge transport materials to reduce injection barriers, facilitate high carrier mobility and adjust charge balance¹⁷⁻¹⁹.

HTMs could effectively transport the holes while blocking the electrons between the hole injection and the emitting layers, which are significant to obtain highly efficient OLEDs. An ideal HTM must possess proper HOMO and LUMO energy levels, outstanding hole mobility,

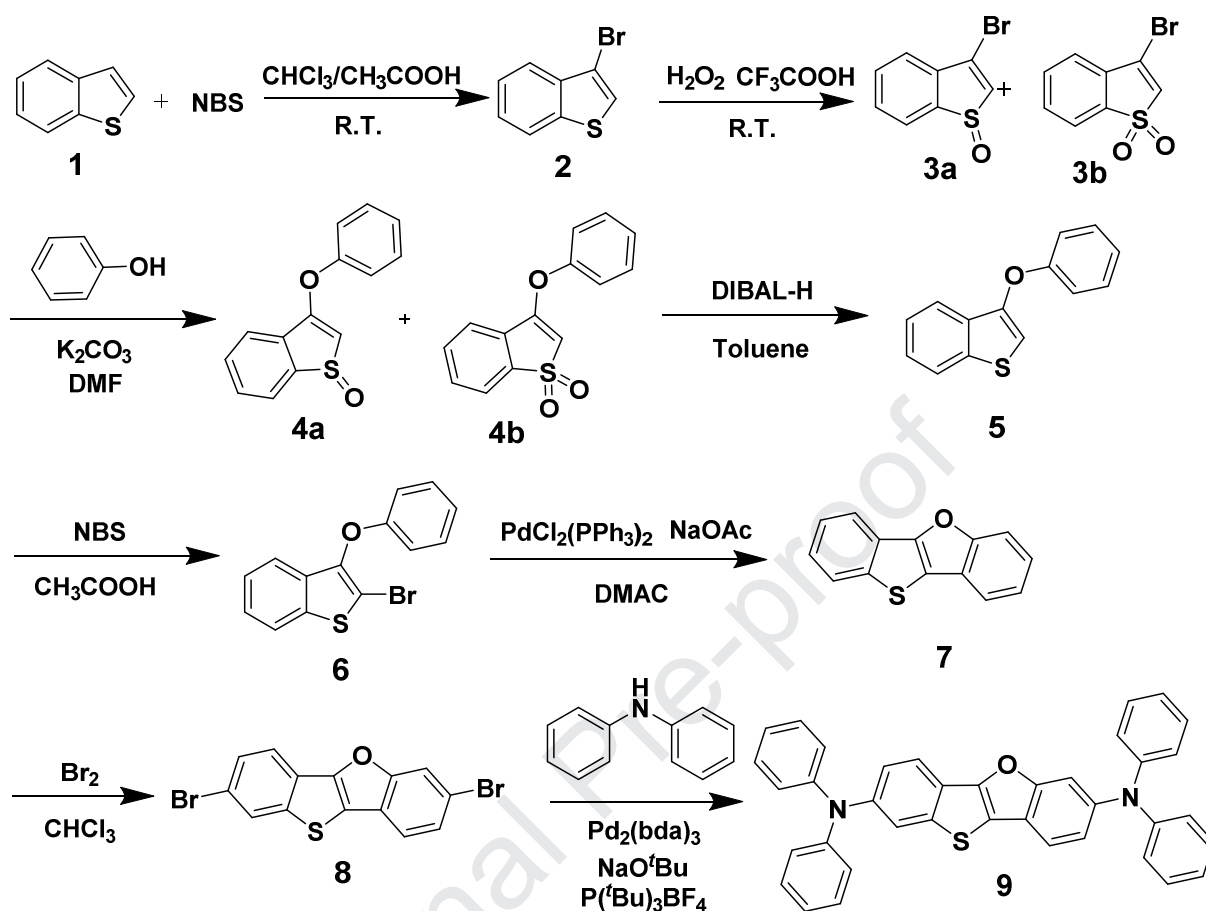
good thermal stability and high triplet energy²⁰⁻²². Triarylamine-type compounds have been generally recognized as excellent hole transporter for OLEDs as well as organic/ perovskite solar cells because of their intrinsic potential to meet those requirements²³⁻²⁵. *N, N'*-bis-(3-methylphenyl)-*N, N'*-bis-phenyl-benzidine (TPD) and *N, N'*-di(naphthalen-1-yl)-*N, N'*-diphenyl-[1, 1'-biphenyl]-4,4'-diamine (NPB) are among the most widely used HTMs due to their outstanding hole-transporting properties, although their low T_g (60 °C for TPD and 95 °C for NPB), and low E_T (2.23 eV for NPB) are obvious defects of them²⁶⁻³⁰. Many Studies on developing better hole transport materials to replace TPD or NPB (or modify their structure) have been reported in the literature. Replacement of biphenyl center in TPD by fluorine derivatives was found to be effective to improve T_g as well as reduce the ionization energy and redox potential. Moreover, the hole mobility is also affected by a change in neutral state and radical cation brought by the torsion angle difference between biphenyl and fused fluorene^{29, 31-32}. Adding a spiro fluorene or triphenylamine group annulated to the central biphenyl of NPB was another strategy to enhance the molecule rigidity and T_g (140 °C) to attain high performance of related OLEDs^{26, 33-34}.

In this contribution, we designed and synthesized a simple arylamine compound, BTBF-DPA, as an effective HTM for OLEDs. In the function of electron acceptors, benzofuran and benzothiophene groups offer excellent stability and high triplet energy since they can decrease the oxidation potential, increase the number of delocalized electrons, and subsequently enhance the HOMO energy level such that the hole carriers are transferred readily^{32, 35-37}. The integration of furan and thiophene adjacent to biphenyl ring strengthen the ability of hole transport and more importantly move the performance of OLEDs to the next level. Green and red PhOLEDs using BTBF-DPA were fabricated to investigate the device performance. Compared with NPB as

reference, green and red PhOLEDs with BTBF-DPA exhibited superior device performance. In addition, blue FOLEDs based on BTBF-DPA were also developed to estimate the potential commercialization, which show better EL performance with low driving voltage and low efficiency roll off at high brightness. What's more, devices lifetime of RGB OLEDs with BTBF-DPA were investigated which showed long lifetime at high brightness. These encouraging results reveal the potential of BTBF core as a promising moiety to develop novel and stable HTMs, and one successful strategy to develop efficient HTMs. Especially, it is worth mentioning that we designed an new and effective approach to successfully synthesizes BTBF³⁸⁻⁴². This is the first demonstration of employing BTBF derivative in OLEDs. Besides, the strong deep blue fluorescence and good solubility of this compound may provide other potential applications in organic optical electronic fields.

2. RESULTS AND DISCUSSION

2.1. Synthesis



Scheme 1. The synthesis route of BTBF-DPA

The molecular structure and synthetic routes of the intermediates and target compound are demonstrated in **Scheme 1**. The target compound was prepared by Buchwald-Hartwig coupling reaction, then purified by flash column chromatography, recrystallized from DCM and methanol and subliming furnace at 280 °C under 1.0×10^{-5} Pa, subsequently, with a final yield of 82.3%. The structures of BTBF-DPA were confirmed by ^1H NMR, ^{13}C NMR and high-resolution mass spectrometry (HRMS). BTBF-DPA are readily soluble in common organic solvents with strong fluorescence.

2.2. Electronic Structure

To get more insights into the potential nature of BTBF-DPA and the difference between BTBF-DPA and NPB, density functional theory (DFT) calculations were performed to simulate the frontier orbitals of HOMO/LUMO distributions and energy levels under the B3LYP/6-31G (d, p) basis set as shown in **Figure 1**. The HOMO of BTBF-DPA is delocalized 46.87% on the BTBF core and the rest 53.13% is located on diphenylamine moiety. While the LUMO is mainly (85.43%) distributed on the BTBF core due to the strong electron negativity of oxygen and sulfur. For NPB, the LUMO only delocalized 6.3% on the biphenyl core, which is completely different from BTBF-DPA.

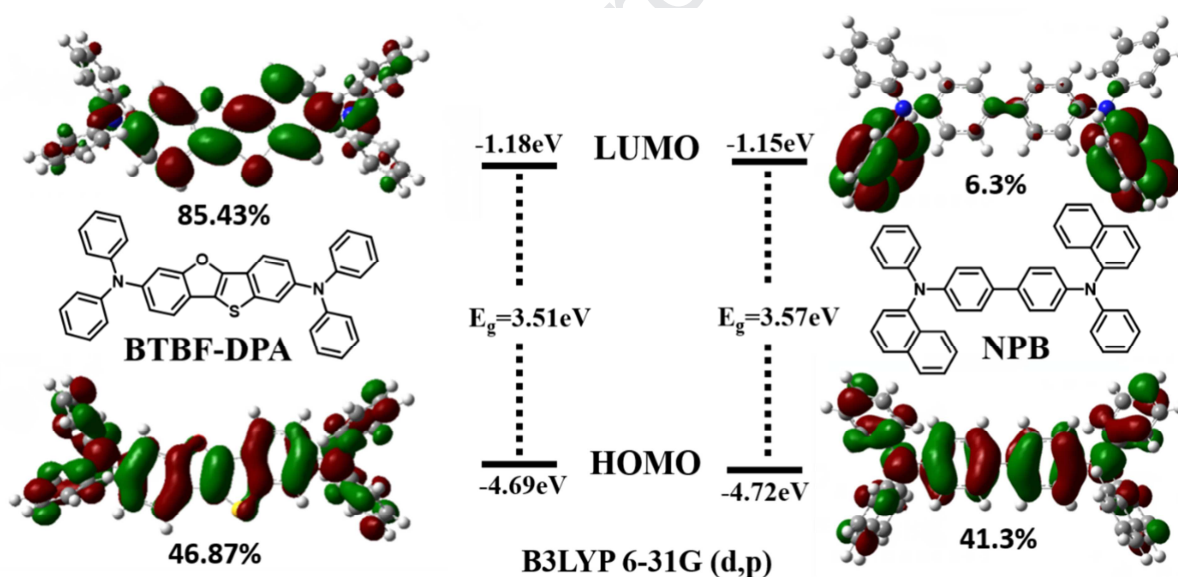


Figure 1. HOMO and LUMO distributions and energy levels of BTBF-DPA and NPB by B3LYP/6-31G (d, p) calculation.

The higher electron density between two nitrogen atoms could bring higher hole transport ability in molecule which was proven by the hole only device later. The energy of the frontier orbitals of

BTBF-DPA is estimated to be -4.69 and -1.18 eV, which are similar to that of NPB, which demonstrated the comparability between BTBF-DPA and NPB in the same device structure.

2.3. Photo-physical Properties

The normalized UV-vis absorption, steady-state photoluminescence (PL) spectra and low temperature (77 K) phosphorescence spectra of **BTBF-DPA** in toluene (1.0×10^{-5} M) and in solid film (deposited under vacuum, 30 nm) are shown in **Figure 2a** and **2b**, respectively. The short-wavelength absorption band at 265 nm belongs to the $\pi-\pi^*$ transition of benzene. The absorption band at nearly 300 nm is associated with the $\pi-\pi^*$ transition and $n-\pi^*$ transition of the triphenylamine-centered moiety. The high intensity absorption band ranging from 350 to 390 nm is attributed to the $\pi-\pi^*$ transition and $n-\pi^*$ of the rigid BTBF unit. The compound indicated an intramolecular charge transfer (ICT) absorption peak at 390 nm in DCM solution and at 401 nm in neat film state. According to the absorption edge, the optical energy gap is calculated to be 3.03 eV. The compound showed strong deep-blue emission with maximum emission peak at 402 nm and 417 nm in DCM solution and neat film, respectively. The PL of neat film is redshifted by 15 nm because of the stronger molecular aggregation effect between molecules, which could also be seen from the long-tailed peak from 468 nm to 612 nm.

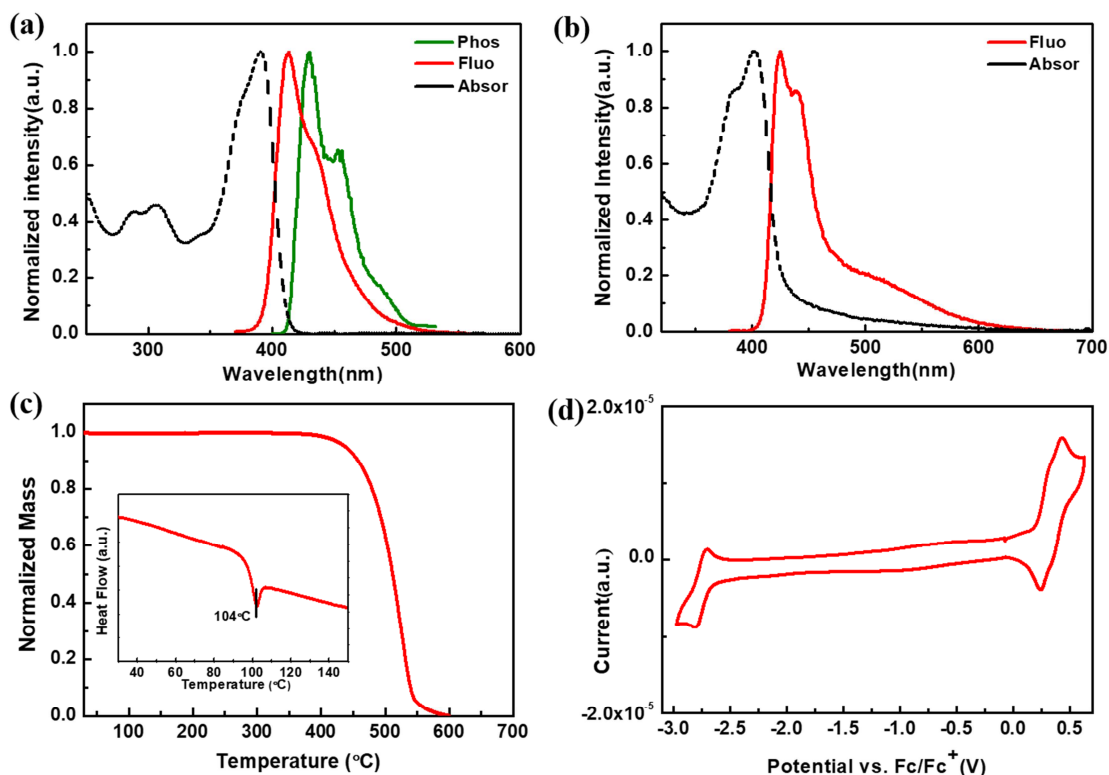


Figure 2. (a) UV-vis absorption, fluorescence and phosphorescence spectra of BTBF-DPA in toluene solution; (b) UV-vis absorption, fluorescence spectra of BTBF-DPA in neat film; (c) TGA and DSC curves of the material BTBF-DPA. Heating rate: 10 °C/min; (d) The CV curve of BTBF-DPA in DMF solution.

Table 1 Material properties of BTBF-DPA and NPB

Compound	Absorption λ_{\max}^a [nm]	Emission λ_{\max}^a [nm]	S_1^b [eV]	T_1^c [eV]	HOMO ^d [eV]	LUMO ^d [eV]	$E_g^{d,e}$ [eV]	T_g^f [°C]	T_d^g [°C]
BTBF-DPA	390	413	3.15	2.99	-5.02	-2.12	2.90/3.03	104	430
NPB ²⁶	345	441	-	2.23	-5.12	-2.05	3.0	95	490

a. Measured in toluene in a concentration of 1.0×10^{-5} M.

b. Estimated from onset of the absorption spectra ($E_g = 1240/\lambda_{\text{onset}}$).

c. Estimated from onset of the low temperature phosphorescent spectra

- d. The HOMO and LUMO energy level is determined from cyclic voltammetry ($E_{\text{HOMO}} = -4.8 - E_{\text{ox}}$, $E_{\text{LUMO}} = -4.8 - E_{\text{red}}$).
- e. The band gap is determined from the film absorption spectra.
- f. Measured by DSC.
- g. Measured by TGA.

Due to the rigid BTBF core, the structural vibrations in the excited states could be suppressed to some extent, resulting in a narrower PL emission which full width of half maximum (FWHM) of 41 nm and 37 nm in toluene solution and neat film, respectively. The triplet energy of BTBF-DPA was determined by the short-wavelength onset of its low temperature (77 K) phosphorescence spectra under nitrogen atmosphere in toluene (1.0×10^{-5} M) solution, which is as high as 2.99 eV¹³.

2.4. Thermal Properties

The thermal properties of BTBF-DPA were investigated by thermogravimetric analysis (TGA) and differential scanning calorimetry analysis (DSC) under nitrogen atmosphere with a heating rate of 10 °C min⁻¹. As shown in **Figure 2c** and **Table 1**, BTBF-DPA showed good thermal stability with the decomposition temperatures (T_d , correspond to 5% weight loss) of 430 °C and glass transition temperature (T_g) of 104°C which is higher than that of NPB (T_g , 95 °C). The higher T_g suggesting better morphological stability of BTBF-DPA compared to NPB. Therefore, BTBF-DPA is expected to be a good HTM owing to its excellent thermal stability behavior.

2.5. Electrochemical Properties

The electrochemical behavior of BTBF-DPA were tested by cyclic voltammograms (CV) using a standard three-electrode electrochemical cell in an electrolyte solution (0.1 M TBAPF₆/DMF, with ferrocene as an external reference. As shown in **Figure 2d** and **Table 1**, the HOMO energy level of BTBF-DPA were calculated to be -5.02 eV, which is higher than that of NPB (-5.12 eV). The corresponding LUMO energy level is calculated to be -2.12 eV. The energetically favorable HOMO energy level of BTBF-DPA is supposed to be further facilitate the hole injection and transport properties from the anode side. Moreover, the shallow LUMO energy level guarantees the efficient electron blocking ability.

2.6. Carrier Transport Ability

To explore the hole mobility of BTBF-DPA, we fabricated hole only devices with a structure of indium-tin oxide (ITO)/1,4,5,8,9,11-hexaazatriphenylene-hexacarbonitrile (HAT-CN, 10 nm)/BTBF-DPA (100 nm)/HAT-CN (10 nm)/Al (100 nm) and ITO/HAT-CN (10 nm)/NPB (100 nm)/HAT-CN (10 nm)/Al (100 nm). The current density vs voltage (J-V) characteristics of the single-carrier devices. The carrier mobility can be calculated based on the $J^{1/2}$ -V curves according to the space-charge-limited current (SCLC) model as **Figure 3** shows. The calculated hole mobility of BTBF-DPA ($3.1 \times 10^{-5} \text{ cm}^2 \text{ V}^{-1} \text{ s}^{-1}$) is about 7 times higher than that of NPB ($4.5 \times 10^{-6} \text{ cm}^2 \text{ V}^{-1} \text{ s}^{-1}$) at the same device structure and conditions.

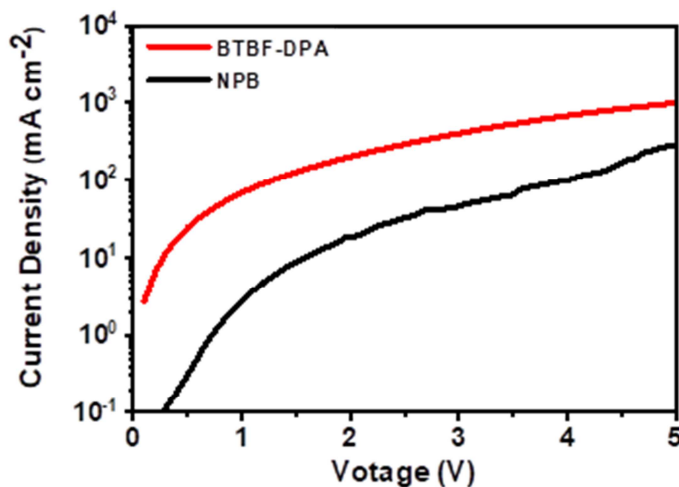


Figure 3. Hole mobility of BTBF-DPA and NPB.

2.7. Electroluminescence Properties

2.7.1 Green PhOLEDs

In order to figure out the potential of BTBF-DPA in device application, we fabricated green PhOLEDs devices using Ir(ppy)₂acac as an emitter. The key device data are summarized in **Table 2**. As shown in **Figure 4b**, the green device structure is ITO/ HAT-CN (5 nm)/ BTBF-DPA (20 nm) or NPB (20 nm)/ Spiro-3-BPF (15 nm)/ DMIC-TRZ : DMIC-Cz : Ir(ppy)₂acac (10:10:1) (15 nm)/ ANT-BIZ (20 nm)/ Liq (1 nm)/ Al (100nm)⁴³. Here in, HAT-CN served as a hole-injection layer and Liq as an electron-injection layer; BTBF-DPA or NPB are employed as HTMs, ANT-BIZ worked as the electron-transporting material, Spiro-3-BPF was used as electron blocking layer (EBL) to facilitate hole injection and block electrons. Ir complex was co-evaporated with DMIC-TRZ and DMIC-CZ to form the emitting layer (EML). The doping ratio of DMIC-TRZ :

DMIC-CZ : Ir(ppy)₂acac complex was 10:10:1. All the details about materials used here were explained in Supporting Information.

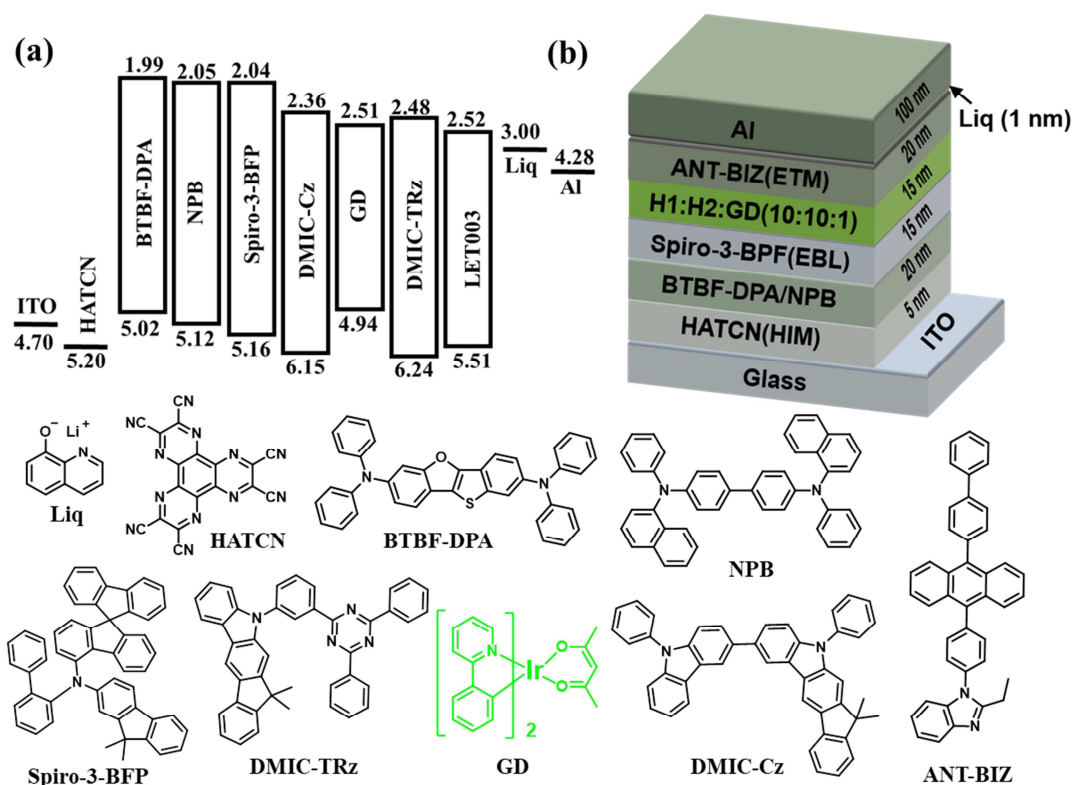


Figure 4. (a) Energy diagram, (b) structure and materials (bottom) used in green PhOLEDs.

This is an exciplex system in which H1 is n-type host and H2 is p-type host. The singlet and triplet energies of exciplex hosts transfer to the singlet and triplet states of iridium complexes through the Foster and Dexter energy transfer, respectively. Then, the singlet excitons of iridium complex could transfer to a triplet state for emission through the intersystem crossing (ISC) process to achieve 100% exciton utilization. The electroluminescent properties of BTBF-DPA and NPB based devices, including current efficiency (CE), power efficiency (PE) and external quantum efficiency (EQE) as well as

the electroluminescence spectra, are demonstrated in **Figure 5** and the key parameters are summarized in **Table 2**.

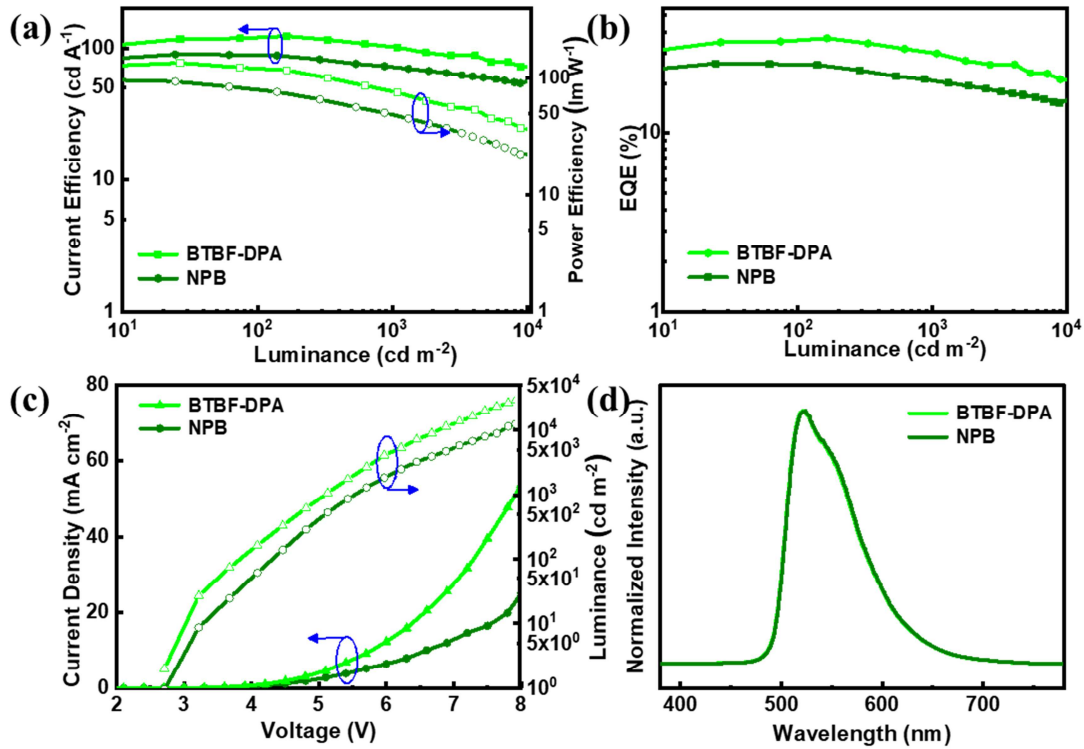


Figure 5. Device characteristics of green PhOLEDs with BTBF-DPA and NPB as HTMs : (a) J-L-P characteristics, (b) EQE-L characteristics, (c) J-V-L characteristics, (d) EL spectra.

The BTBF-DPA based device exhibit stable green emission at the peak of 523 nm with CIE of (0.34, 0.61), whereas NPB based device emits the same green light characteristics. The green devices based on BTBF-DPA show an extremely low turn-on voltage (V_{on} voltage at 1 cd m^{-2}) as low as 2.4 V which is the same as that of NPB based green device.

Table 2. Performance of Green PhOLEDs.

Green	V_{on}	CE(cd A^{-1})	PE(lm W^{-1})	EQE(%)	CIE
Pospho-	(V)	max @ 1000 cd m^{-2}	max @ 1000 cd m^{-2}	max @ 1000 cd m^{-2}	(x,y)

rescence		/10000cd m ⁻²		/10000cd m ⁻²		/10000cd m ⁻²	
BTBF	2.4	123.6	102.8/72.1	136.6	77.8/36.8	34.1	28.4/20.0 (0.34, 0.61)
NPB	2.4	89.7	71.2/55.7	96.8	43.4/28.8	24.7	19.6/15.3 (0.34, 0.61)

In detail, as shown in **Table 2** and **Figure 5**, NPB based device showed a peak EQE of 27.4%, a maximum CE of 89.7 cd A⁻¹, and a maximum power efficiency (PE) of 96.8 lm W⁻¹. With enhanced hole mobility and high T_g , the device based on BTBF-DPA exhibited a peak EQE of 34.1%, a maximum CE of 123.6 cd A⁻¹, and a maximum PE of 136.6 lm W⁻¹. The significant enhancement in the efficiency of the BTBF-DPA based green device can be attributed to better balanced charge recombination at the emitting layer due to the outstanding hole mobility of BTBF-DPA. Furthermore, devices based on BTBF-DPA could reach very high brightness at low voltage which means higher luminous efficacy and lower energy consumption than the devices based on NPB.

2.7.2 Red PhOLEDs

We also fabricated red PhOLEDs to further demonstrate the universality of BTBF-DPA as HTM. The device structure is the same as green PhOLEDs except the dopant is replaced by Irpql-acac, demonstrated in Supporting Information S1. The electroluminescent properties of BTBF-DPA based red phosphorescent device are shown in **Figure 6** and the key parameters are summarized in **Table 3**.

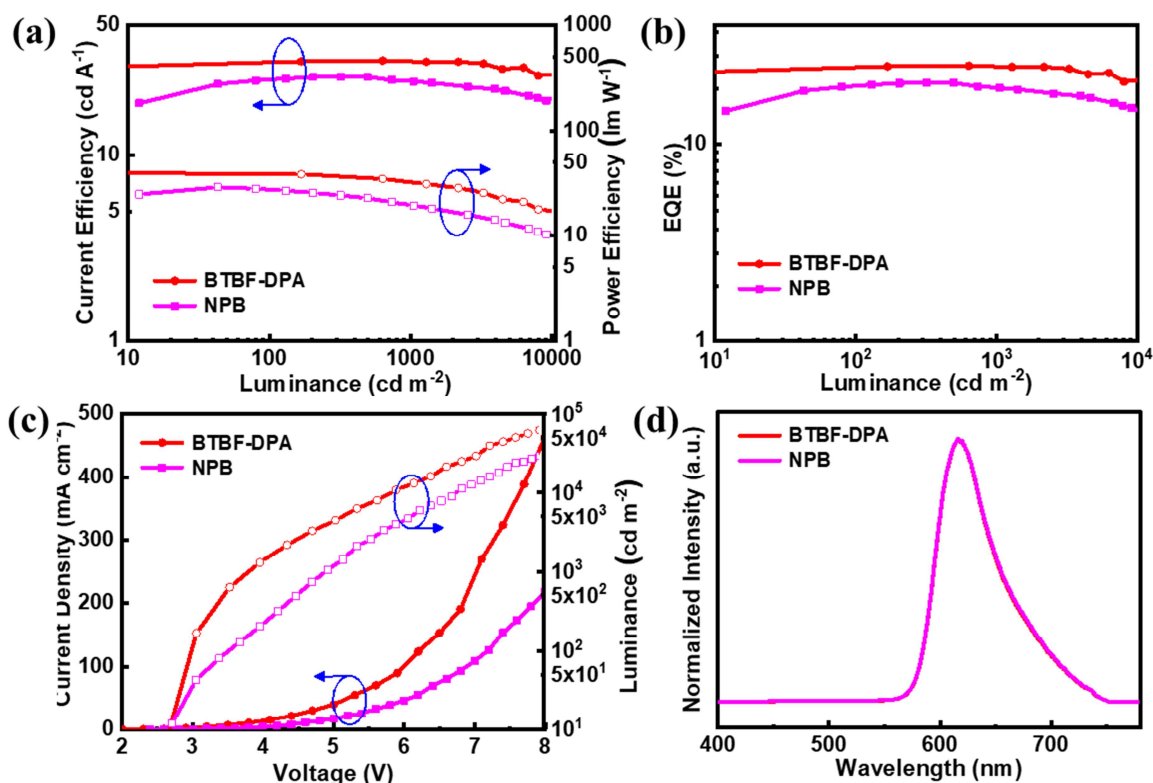


Figure 6. Device characteristics of red PhOLEDs with BTBF-DPA and NPB as HTMs : (a) J-L-P characteristics, (b) EQE-L characteristics, (c) J-V-L characteristics, (d) EL spectra.

Table 3. Performance of Green/red/blue PhOLEDs based on BTBF-DPA as HTM.

Red	V_{on}	CE(cd A ⁻¹)	PE(lm W ⁻¹)	EQE(%)	CIE
Pospho- rescence	(V)	max @1000cd m ⁻² /10000cd m ⁻²	max @1000cd m ⁻² /10000cd m ⁻²	max @1000cd m ⁻² /10000cd m ⁻²	(x,y)
BTBF	2.3	32.3 31.8/27.4	40.1 31.2/17.9	24.9 24.6/21.1	(0.65, 0.34)
NPB	2.3	26.3 24.9/19.7	29.1 19.5/10.4	20.4 19.2/15.6	(0.65, 0.34)

The BTBF-DPA based red device exhibit deep red emission peaking at 624 nm with CIE of (0.65, 0.34) and a low turn-on voltage (V_{on} voltage at 1 cd m^{-2}) as 2.3 V. As shown in **Table 3** and **Figure 6**, the maximum EQE, CE, and PE of BTBF-DPA based red POLEDs are 24.9%, 32.3 cd A^{-1} , and 40.1 lm W^{-1} . respectively. At high brightness of 1000 cd m^{-2} , the EQE, CE and PE of them are 24.6%, 31.8 cd A^{-1} , and 31.2 lm W^{-1} . The efficiency roll-off of BTBF-DAP based device is 1.2% at 1000 cd m^{-2} which is much smaller than 5.9% of NPB's. What matters most is the PE of BTBF-DPA based device is 37.8% higher than NPB's. The results of higher PE and lower efficiency roll-off of BTBF-DPA based device declare that BTBF-DPA could performs much better than NPB in commercial applications of red OLEDs.

2.7.3 Blue FOLEDs

In order to further evaluate the potential of BTBF-DPA as HTM in commercialized blue fluorescent (FOLEDs) system, we tested the performance of blue FOLEDs based ITO/HAT-CN(5 nm)/ NPB (80 nm)/ TPN-DPF (10 nm)/ BH: BD (20 nm)/ ATN-BIZ (60 nm)/ Liq (1 nm)/ Al (100 nm). Here, ITO is used as anode; HATCN is the hole-injecting layer; BTBF-DPA or NPB serves as the HTMs; TPN-DPF used as electron blocking layer; the emitting layer is composed of BH and BD (ratio 96 : 4); ATN-BIZ works as the electron-transporting layer, Liq is the electron-injecting layer. The device performance data are summarized in **Table 4**.

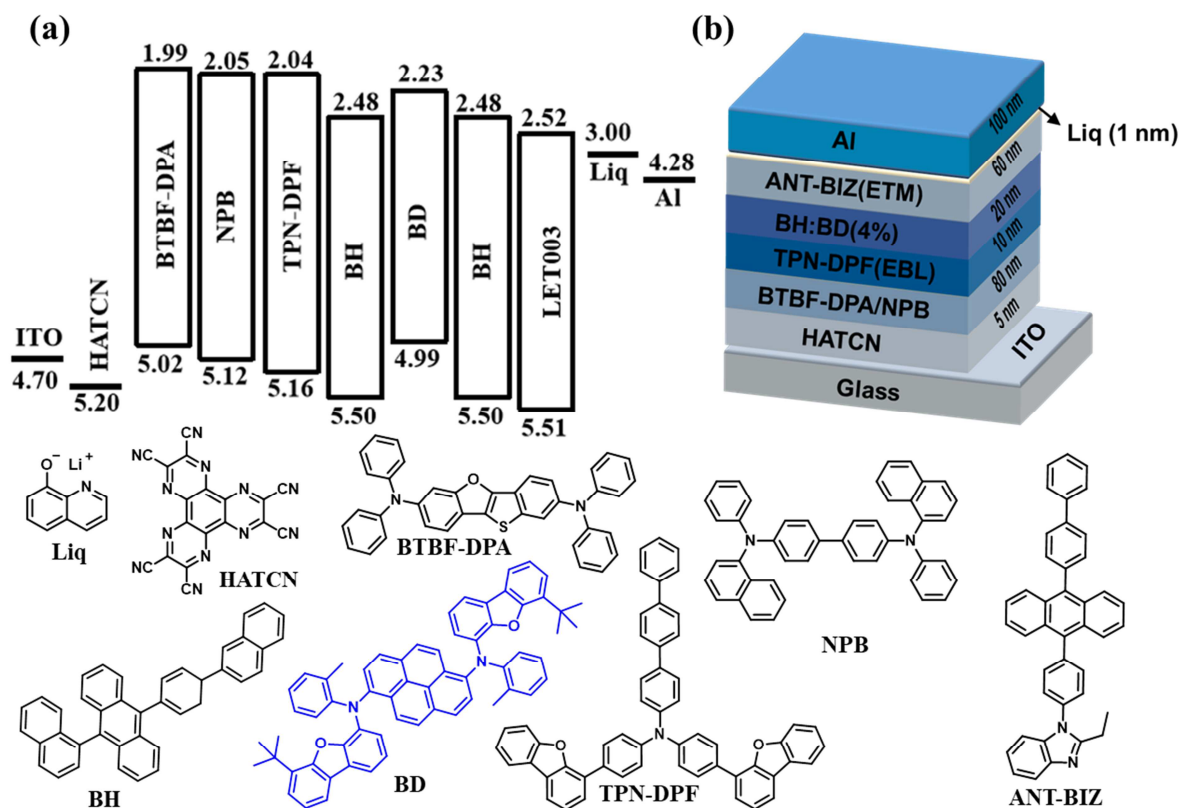


Figure 7. (a) Energy diagram, (b) Device structure and materials used in blue FOLEDs.

The BTBF-DPA based device exhibits stable blue emission peaking at 463 nm with CIE of (0.15, 0.09), whereas NPB based device emit the same blue light with the same CIE of (0.15, 0.09). The devices show the same turn-on voltage (V_{on} voltage at 1 cd m^{-2}) as low as 2.8 V. As shown in **Table 4** and **Figure 8**, the maximum EQE, CE, and PE of BTBF-DPA based device are 4.8%, 4.0 cd A^{-1} , and 4.2 lm W^{-1} , while the device based on NPB exhibited 5.1%, 4.3 cd A^{-1} , and 4.0 lm W^{-1} , respectively. However, the EQE, CE and PE of both of these devices at 10000 cd m^{-2} are 4.1%, 3.4 cd A^{-1} , and 2.0 lm W^{-1} and 4.1%, 3.4 cd A^{-1} , and 1.8 lm W^{-1} , respectively. It is clear to see that BTBF-DPA based blue

device possess better performance than the reference one at high luminescence owing to its higher mobility and super triplet energy.

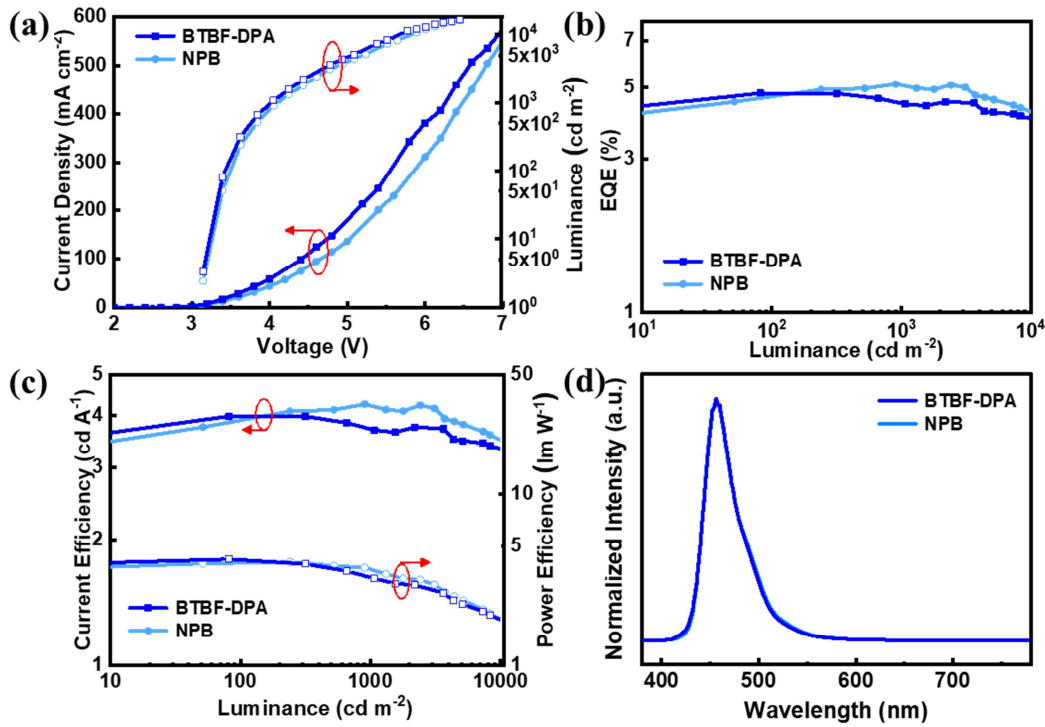


Figure 8. Device characteristics of blue FOLEDs with BTBF-DPA and NPB as HTMs : (a) J-V-L characteristics, (b) EQE-L characteristics, (c) J-L-P characteristics, (d) EL spectra.

Table 4. Performance of blue FOLEDs

Blue Fluorescence	V_{on} (V)	$CE(cd A^{-1})$ max @1000cd m ⁻² /10000cd m ⁻²	$PE(lm W^{-1})$ max @1000cd m ⁻² /10000cd m ⁻²	$EQE(\%)$ max @1000cd m ⁻² /10000cd m ⁻²	CIE (x,y)
BTBF	2.8 4.0	3.7/3.4	4.2 3.3/2.0	4.8 4.5/4.1	(0.15, 0.09)
NPB	2.8 4.3	4.1/3.4	4.0 3.4/1.8	5.1 5.0/4.1	(0.15, 0.09)

In order to enhance the EQE of BTBF-DPA based device to over 5% which is the limitation of blue fluorescence OLEDs. We further optimized the device structure. The

hole transport ability of BTBF-DPA thin film of 80 nm is 7 times higher than that of NPB according to the hole only device, so it may cause the difference of charge balance in former blue FOLEDs which can be seen from the device performance. Here, we increased the thickness of BTBF-DPA in blue FOLEDs from 80 nm to 120 nm to get an improved performance, owing to more balanced charge transport ability. The blue FOLEDs with 120 nm of BTBF-DPA exhibited better EQE, CE, PE and efficiency roll-off. The maximum of which are 5.2%, 4.7 cd A^{-1} , 4.9 lm W^{-1} and the efficiency roll-off is 3.9% at 1000 cd m^{-2} and 9.8% at 10000 cd m^{-2} . These results showed in **Figure 9** and **Table 5**, which are comparable to reported results⁴⁴⁻⁴⁵. The CIE changed from (0.15, 0.09) to (0.15, 0.10) owing to the carriers recombination zone become broaden resulting from the 40 nm thicker of BTBF-DPA as HTM. The consequences indicate that BTBF-DPA can be adopted as an efficient HTM in blue FOLEDs.

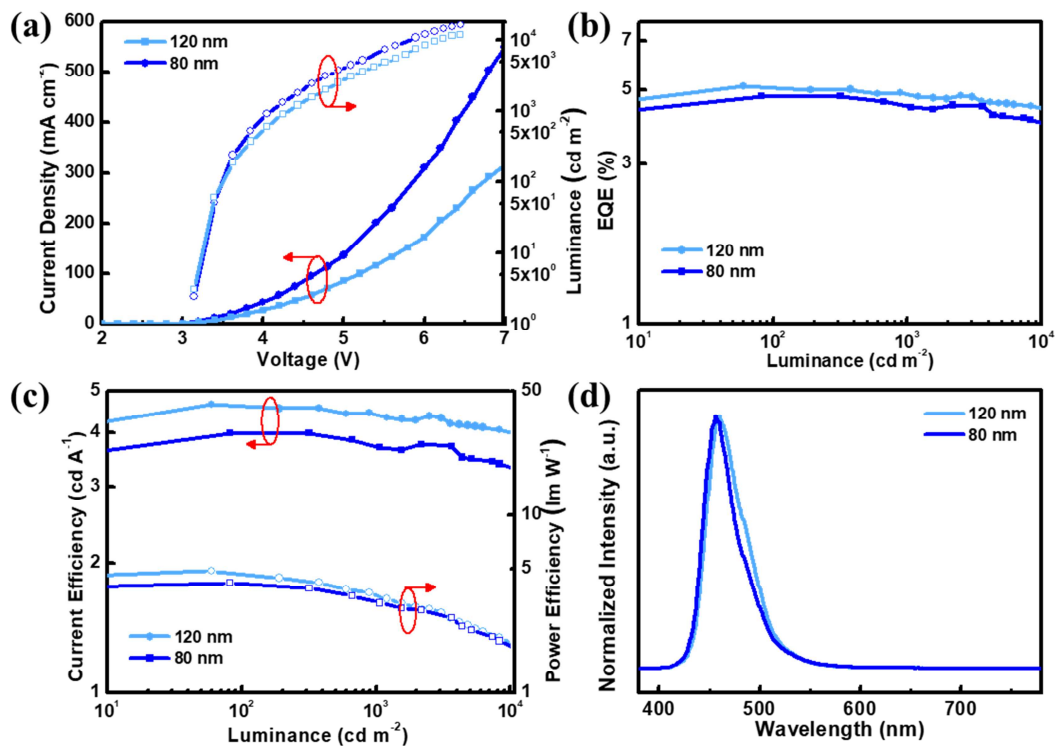


Figure 9. Device performances of blue FOLEDs based on 80nm and 120nm of BTBF-DPA: (a) J-V-L characteristics, (b) EQE-L characteristics, (c) J-L-P characteristics, (d) EL spectra.

Table 5. Performance of 80nm and 120 nm BTBF-DPA based blue FOLEDs

Blue	V_{on}	$CE(cd A^{-1})$	$PE(lm W^{-1})$	$EQE(\%)$	CIE
Fluorescence	(V) max	@1000cd m ⁻² /10000cd m ⁻²	max @1000cd m ⁻² /10000cd m ⁻²	max @1000cd m ⁻² /10000cd m ⁻²	(x,y)
80nm	2.8 4.0	3.7/3.4	4.2 3.3/2.0	4.8 4.5/4.1	(0.15, 0.09)
120nm	2.8 4.7	4.5/4.2	4.9 3.7/2.1	5.2 4.9/4.6	(0.15, 0.10)

2.7.4 Lifetime of OLEDs

Device stability of BTBF-DPA based RGB devices were evaluated by collecting operation time dependent luminance at an initial luminance of 10000 cd m⁻², 10000 cd m⁻² and 5000 cd m⁻² as supplementary information, respectively. Constant current mode lifetime test was carried out for the lifetime evaluation in glovebox without encapsulation. Lifetime data in **Figure 10** verifies that life-time of RGB OLEDs are $T_{99} = 70$ h at 10000 cd m⁻², $T_{70} = 60$ h at 10000 cd m⁻², $T_{80} = 125$ h at 5000 cd m⁻². For red PhOLEDs, the device is extremely stable owing to the low driving voltage and balanced carrier transportation. For green PhOLEDs, the green emitter is not as stable as red emitter and the driving voltage is higher than that of green device, so the stability is not as good as green device under the condition of 10000 cd m⁻². In blue FOLEDs, the blue emitter is very stable which was reported by a patent demonstrated in Supporting Information. Under the condition of 5000 cd m⁻², T_{80} is 125h which is an excellent performance for

blue device with CIE_y below 0.1, and BTBF-DPA as a stable and efficient HTM plays a significant role in this system. These results reveal that BTBF-DAP could perform well as HTM in RGB OLEDs.

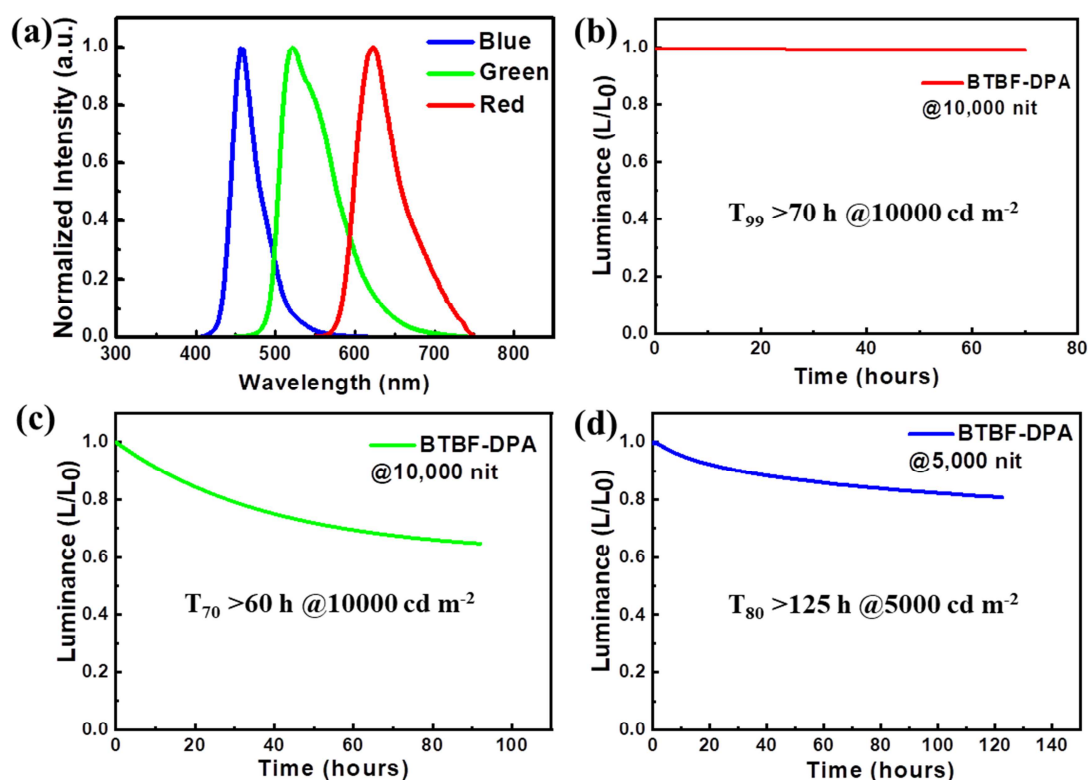


Figure 10. Device performances of RGB OLEDs based on BTBF-DPA: (a) EL characteristics of RGB OLEDs, (b) Life-time of red PhOLED, (c) Life-time of green PhOLED, (d) Life-time of blue FOLED with 120nm BTBF-DPA.

3. CONCLUSION

In conclusion, we developed a novel HTM, BTBF-DPA, with proper HOMO, high mobility and high E_T by introducing a new and electron rich mioty-BTBF into arylamine system. Using BTBF-DPA, we successfully accomplished efficient and stable RGB OLEDs exhibiting maximum PE of 40.1 lm W⁻¹, 136.6 lm W⁻¹ and 4.9 lm W⁻¹, EQE of 24.9%, 34.1% and 5.2%, and the efficiency roll-off of them are 16.7% at 1000 cd m⁻²,

1.2% at 1000 cd m⁻² and 11.5% at 10000 cd m⁻², respectively. As a reference, NPB based RGB PhOLED device only has maximum PE of 29.1 lm W⁻¹, 96.8 lm W⁻¹ and 4.0 lm W⁻¹, EQE of 20.4%, 24.7%, 5.1%, and the efficiency roll-off of them are 20.6% at 1000 cd m⁻², 5.9% at 1000 cd m⁻², 19.6% at 10000 cd m⁻², which are much lower than BTBF-DPA based OLEDs, respectively. The lifetime of RGB OLEDs with BTBF-DPA were investigated, which are $T_{99} = 70$ h at 10000 cd m⁻², $T_{70} = 60$ h at 10000 cd m⁻², $T_{80} = 125$ h at 5000 cd m⁻². These results indicate that BTBF-DPA is a promising HTM for improving the PE, EQE and the efficiency roll-off of RGB OLEDs. In the future, phosphorescent and/or fluorescent OLEDs with high power efficiency, low driving voltage, low efficiency roll-off and long lifetime can be achieved by employing our newly developed HTM because of its appropriate energy level, fine hole mobility and very high E_T of 2.99 eV. In addition, our molecular design strategy and new rigid core BTBF demonstrated in this work will contribute to promote the commercialization of phosphorescent and/or fluorescent OLEDs. In the next step, we will try to increase the T_g of HTMs based on BTBF derivatives by connecting high weight arylamine groups or introducing more heteroatom into aromatic conjugation system. This will continually contribute to enhance the stability of materials as well as devices. We believe that BTBF derivatives could also perform well in TADF OLEDs system, organic photovoltaics (OPVs), perovskite light-emitting diodes (PLEDs) and quantum dots light-emitting diodes (QLEDs) considering its outstanding stability and solvability.

4. EXPERIMENT SECTION

Synthesis information

Synthesis of 3-bromobenzo[b]thiophene 2

Benzothiophene (3.35 g, 25 mmol) and N-Bromosuccinimide (NBS) (5.34 g, 30 mmol) were dissolved in a mixture of CHCl_3 (200 mL) and CH_3COOH (200 mL) at 0 °C and stirred for 2h before reacted at room temperature for 12 h. After reaction, saturated sodium thiosulfate solution (100 ml) and saturated sodium carbonate (100 ml) were added to remove excess NBS. The mixture was washed with water (100 mL) and extracted with DCM. The solvent was evaporated and the residual crude product was purified by column chromatography on silica gel using PE as an eluent to afford **2** (7.69 g, 98.6%) as yellow oil. $^1\text{H NMR}$ (300 MHz, CDCl_3) δ 7.86 (d, $J = 8.6$ Hz, 1H), 7.53 – 7.38 (m, 2H).

Synthesis of compounds of 3, 4 and 5

3-Bromobenzo[b]thiophene (1.77 g, 8.4 mmol) was added into CHCl_3 (120 mL) and CF_3COOH (120 mL) was put in the mixture followed by stirring for 6 minutes at room temperature. Then H_2O_2 (10 g) was added in the mixture and stirred for 20 h at room temperature. After reaction, saturated sodium carbonate (50 mL), saturated sodium bicarbonate (50 mL) and water (50 mL) were added for washing, and then the mixture was extracted by CHCl_3 (150 ml) and concentrated under reduced pressure. The resulting crude product was purified by silica gel column chromatography using PE: DCM (1: 1, v/v) as an eluent. A yellow oil (1.83 g, 7.74 mmol) was obtained, which represents a mixture of 3-bromobenzo[b]thiophene-1-oxide and 3-bromobenzo[b]thiophene-1,1-dioxide as **3**. This product was used in the next reaction without further separation of these two compounds. The mixture was added into dry DMF (30 ml) with phenol (1.45 g, 15.5 mmol) and potassium carbonate (2.14 g, 15.5 mmol) and stirred at 70 °C for 15 h before water (3×50 mL) was put into the mixture. Then the mixture was extracted by CHCl_3 (150mL) and concentrated. The resulting crude product was purified by silica gel column chromatography using DCM as an eluent, and 1.86 g (7.46 mmol) yellow oil which is a mixture

of 3-phenoxybenzo[*b*]thiophene-1-oxide and 3-phenoxybenzo[*b*]thiophene-1, 1-dioxide were obtained as **4**. Without further purification, the mixture was added into toluene (80 ml) with diisobutylaluminium hydride (12.4 mL, 18.6 mmol) at 0 °C and then stirred at 65 °C for 20 h. After reaction, toluene was removed under reduced pressure, then 2 M NaOH solution (30 mL) was added at 0 °C and extracted with DCM. The organic phase was dried and concentrated to get crude product as yellow oil which was then passed by silica gel column chromatography using PE as an eluent to afford **5** (1.01 g, 59.9%) as yellow oil. ¹H NMR (300 MHz, CDCl₃) δ 7.84 (d, J = 1.3 Hz, 1H), 7.78 (d, J = 7.7 Hz, 1H), 7.35 – 7.48 (m, 5H), 7.19 (dd, J = 4.2, 2.4 Hz, 3H), 6.72 (s, 1H). ¹³C NMR (300 MHz, CDCl₃) δ 157.74, 148.03, 138.14, 132.37, 129.90, 125.33, 124.26, 123.61, 123.23, 121.21, 118.12, 107.16.

*Synthesis of 2-Bromo-3-Phenoxybenzo[*b*]thiophene 6*

3-Phenoxybenzo[*b*]thiophene (1.01 g, 4.48 mmol) and NBS (0.96 g, 5.37 mmol) were dissolved into CH₃COOH (120 mL) stirred at 55 °C for 12 h. After reaction, saturated sodium bicarbonate (100 mL) was added to react with excess CH₃COOH and then retracted with DCM. The organic phase was dried and concentrated to yield **6** (1.26 g, 92.1%) as a white solid. ¹H NMR (300 MHz, CDCl₃) δ 7.72 (d, J = 7.9 Hz, 1H), 7.46 (d, J = 7.9 Hz, 1H), 7.34 (m, J = 10.6, 8.1, 1.1 Hz, 3H), 7.06 (t, J = 7.4 Hz, 1H), 6.96 (dd, J = 8.1, 1.5 Hz, 2H).

*Synthesis of Benzo[4,5]thieno[3,2-*b*]benzofuran (BTBF) 7*

2-Bromo-3-Phenoxybenzo[*b*]thiophene (1.26 g, 4.13 mmol), NaOAc (0.53 g, 8.3 mmol) and PdCl₂(PPh₃)₂ (0.14 g, 0.2 mmol) were added into a pressure flask with *N,N*-dimethylacetamide (30 mL) under nitrogen atmosphere and stirred at 145 °C for 12 h. After reaction, 2 M HCl (12 mL) and saturated NaCl solution (100 mL) were added to the mixture and extracted with EA :

hexane (1:1, v/v)(6 × 30 mL). The combined organic layer was dried over MgSO₄ and concentrated to pass the column chromatography on silica gel using PE as an eluent to afford white solid **7** (0.83 g, 89.3%). ¹H NMR (300 MHz, CDCl₃) δ 8.02 (d, J = 8.2 Hz, 1H), 7.89 (d, J = 8.0 Hz, 1H), 7.74 (dd, J = 7.3, 1.6 Hz, 1H), 7.66 (dd, J = 7.0, 1.8 Hz, 1H), 7.44 – 7.53 (d, 1H), 7.44 – 7.32 (m, 3H).

Synthesis of 2,7-Dibromobenzo[4,5]thieno[3,2-b]benzofuran (BTBF-2Br) 8

BTBF (2.26 g, 10 mmol) was dissolved in dry CHCl₃ (100 mL) and stirred at 0 °C. Liquid bromine (4.0 g, 25.0 mmol) in dry CHCl₃ (30 mL) was added dropwise into the above BTBF solution at 0 °C for 30 min. The mixture was stirred at room temperature for 24 h before washed by saturated sodium thiosulfate solution (50 mL). The product was extracted with DCM (3 × 30 mL). The combined organic phase was collected, dried over MgSO₄ and concentrated. The crude product was purified by column chromatography on silica gel using PE as an eluent to afford **BTBF-2Br 8** (3.45 g, 90%) as white solid. ¹H NMR (400 MHz, CDCl₃) δ 8.02 (d, J = 1.4 Hz, 1H), 7.85 (d, J = 8.5 Hz, 1H), 7.81 (d, J = 1.5 Hz, 1H), 7.61 – 7.56 (m, 2H), 7.49 (dd, J = 8.3, 1.7 Hz, 1H).

Synthesis of 2,7-Bis(diphenylamino)-benzo[4,5]thieno[3,2-b]benzofuran (BTBF-DPA) 9

A mixture of BTBF-2Br (1.92 g, 5 mmol), diphenylamine (2.03 g, 12 mmol), sodium *tert*-butoxide (1.44 g, 15 mmol), tris(dibenzylideneacetone) dipalladium (0) (0.18 g, 0.2 mol, 4 mol%) and tri-*tert*-butylphosphine tetrafluoroborate (0.17 g, 0.6 mmol) were dissolved in methylbenzene (50 mL) and heated at 120 °C for 12 h under nitrogen. After cooling to room temperature, the solvent was removed by rotary evaporation under vacuum, and then cold water was added to the mixture and extracted with DCM (3 × 30 mL). The combined organic phase

was collected, filtered and dried over by MgSO_4 . The crude product was purified by column chromatography on silica gel using PE/DCM (3:1, v/v) as eluent to afforded **BTBF-DAP 9** (2.32 g, 82.3%). $^1\text{H NMR}$ (500 MHz, DMSO) δ 7.84 (d, $J = 8.6$ Hz, 1H), 7.77 (d, $J = 8.5$ Hz, 1H), 7.65 (d, $J = 1.9$ Hz, 1H), 7.35 – 7.27 (m, 9H), 7.13 (dd, $J = 8.6, 2.0$ Hz, 1H), 7.09 – 7.03 (m, 11H), 7.01 (dd, $J = 8.5, 1.9$ Hz, 1H). $^{13}\text{C NMR}$ (500 MHz, CDCl_3) δ 159.79, 153.06, 148.02, 147.88, 145.61, 145.36, 143.10, 129.53, 129.47, 124.55, 124.42, 123.25, 123.10, 122.41, 120.73, 120.61, 119.82, 119.75, 119.39, 119.17, 117.59, 108.43. **HRMS** (m/z): $[\text{M}+\text{H}]^+$ calcd for $\text{C}_{38}\text{H}_{27}\text{N}_2\text{O}_5$, 559.1799; Found $[\text{M}+\text{H}]^+$: 559.1855.

ASSOCIATED CONTENT

Supporting Information

The Supporting Information is available free of charge via the Internet at <http://pubs.acs.org>.”

AUTHOR INFORMATION

Corresponding Author

* E-mail: menghong@pku.edu.cn

Notes

The authors declare no competing financial interest.

ACKNOWLEDGMENT

This work was financially supported by the Guangdong Key Research Project (No. 2019B010924003), Shenzhen Engineering Research Center (Shenzhen development and reform commission [2018]1410), Shenzhen Peacock Plan (KQTD2014062714543296), Shenzhen Science and Technology research grant (JCYJ20180302153451987, JCYJ20180302153514509),

the Guangdong International Science Collaboration Base (2019A050505003). Thanks for Dr. Junpeng He's instruction and revision work about this manuscript.

REFERENCES

- (1) Tang, C. W.; VanSlyke, S. A. Organic electroluminescent diodes. *Appl Phys Lett* **1987**, *51* (12), 913-915, DOI: 10.1063/1.98799.
- (2) D'Andrade, B.; Adamovich, V.; Hewitt, R.; Hack, M.; Brown, J. J. In *Phosphorescent organic light-emitting devices for solid-state lighting*, Organic Light-emitting Materials & Devices IX, 2005.
- (3) Uoyama, H.; Goushi, K.; Shizu, K.; Nomura, H.; Adachi, C. J. N. Highly efficient organic light-emitting diodes from delayed fluorescence. *Nature* **2012**, *492* (7428), 234-238.
- (4) Ai, X.; Evans, E. W.; Dong, S.; Gillett, A. J.; Guo, H.; Chen, Y.; Hele, T. J. H.; Friend, R. H.; Li, F. Efficient radical-based light-emitting diodes with doublet emission. *Nature* **2018**, *563* (7732), 536-540, DOI: 10.1038/s41586-018-0695-9.
- (5) Cai, X.; Su, S.-J. Marching Toward Highly Efficient, Pure-Blue, and Stable Thermally Activated Delayed Fluorescent Organic Light-Emitting Diodes. *Adv Funct Mater* **2018**, *28* (43), DOI: 10.1002/adfm.201802558.
- (6) Liu, W.; Chen, J.-X.; Zheng, C.-J.; Wang, K.; Chen, D.-Y.; Li, F.; Dong, Y.-P.; Lee, C.-S.; Ou, X.-M.; Zhang, X.-H. Novel Strategy to Develop Exciplex Emitters for High-Performance OLEDs by Employing Thermally Activated Delayed Fluorescence Materials. *Adv Funct Mater* **2016**, *26* (12), 2002-2008, DOI: 10.1002/adfm.201505014.
- (7) Tang, X.; Bai, Q.; Shan, T.; Li, J.; Gao, Y.; Liu, F.; Liu, H.; Peng, Q.; Yang, B.; Li, F.; Lu, P. Efficient Nondoped Blue Fluorescent Organic Light-Emitting Diodes (OLEDs) with a High

External Quantum Efficiency of 9.4% @ 1000 cd m⁻² Based on Phenanthroimidazole–Anthracene Derivative. *Adv Funct Mater* **2018**, 28 (11), DOI: 10.1002/adfm.201705813.

(8) Kim, S.-Y.; Jeong, W.-I.; Mayr, C.; Park, Y.-S.; Kim, K.-H.; Lee, J.-H.; Moon, C.-K.; Brütting, W.; Kim, J.-J. Organic Light-Emitting Diodes with 30% External Quantum Efficiency Based on a Horizontally Oriented Emitter. *Adv Funct Mater* **2013**, 23 (31), 3896-3900, DOI: 10.1002/adfm.201300104.

(9) Li, W.; Pan, Y.; Xiao, R.; Peng, Q.; Zhang, S.; Ma, D.; Li, F.; Shen, F.; Wang, Y.; Yang, B.; Ma, Y. Employing ~100% Excitons in OLEDs by Utilizing a Fluorescent Molecule with Hybridized Local and Charge-Transfer Excited State. *Adv Funct Mater* **2014**, 24 (11), 1609-1614, DOI: 10.1002/adfm.201301750.

(10) Lin, T. A.; Chatterjee, T.; Tsai, W. L.; Lee, W. K.; Wu, M. J.; Jiao, M.; Pan, K. C.; Yi, C. L.; Chung, C. L.; Wong, K. T.; Wu, C. C. Sky-Blue Organic Light Emitting Diode with 37% External Quantum Efficiency Using Thermally Activated Delayed Fluorescence from Spiroacridine-Triazine Hybrid. *Adv Mater* **2016**, 28 (32), 6976-83, DOI: 10.1002/adma.201601675.

(11) Wu, T.-L.; Huang, M.-J.; Lin, C.-C.; Huang, P.-Y.; Chou, T.-Y.; Chen-Cheng, R.-W.; Lin, H.-W.; Liu, R.-S.; Cheng, C.-H. Diboron compound-based organic light-emitting diodes with high efficiency and reduced efficiency roll-off. *Nature Photon* **2018**, 12 (4), 235-240, DOI: 10.1038/s41566-018-0112-9.

(12) Xu, Y.; Liang, X.; Zhou, X.; Yuan, P.; Zhou, J.; Wang, C.; Li, B.; Hu, D.; Qiao, X.; Jiang, X.; Liu, L.; Su, S. J.; Ma, D.; Ma, Y. Highly Efficient Blue Fluorescent OLEDs Based on Upper

Level Triplet-Singlet Intersystem Crossing. *Adv Mater* **2019**, *31* (12), e1807388, DOI: 10.1002/adma.201807388.

(13) Ahn, D. H.; Kim, S. W.; Lee, H.; Ko, I. J.; Karthik, D.; Lee, J. Y.; Kwon, J. H. Highly efficient blue thermally activated delayed fluorescence emitters based on symmetrical and rigid oxygen-bridged boron acceptors. *Nature Photon* **2019**, *13* (8), 540-546, DOI: 10.1038/s41566-019-0415-5.

(14) Udagawa, K.; Sasabe, H.; Igarashi, F.; Kido, J. Simultaneous Realization of High EQE of 30%, Low Drive Voltage, and Low Efficiency Roll-Off at High Brightness in Blue Phosphorescent OLEDs. *Adv Opt Mater* **2016**, *4* (1).

(15) Murawski, C.; Fuchs, C.; Hofmann, S.; Leo, K.; Gather, M. C. Alternative p-doped hole transport material for low operating voltage and high efficiency organic light-emitting diodes. *Appl Phys Lett* **2014**, *105* (11), 113303.

(16) Caroline, M.; Karl, L.; Gather, M. C. Efficiency roll-off in organic light-emitting diodes. *Adv Mater* **2013**, *25* (47), 6801-6827.

(17) Park, M. S.; Lee, J. Y. Indolo Acridine-Based Hole-Transport Materials for Phosphorescent OLEDs with Over 20% External Quantum Efficiency in Deep Blue and Green. *Chem Mater* **2011**, *23* (19), 4338-4343, DOI: 10.1021/cm201634w.

(18) Tai, P.; Yu, Y.; Yu, L.; Dongge, M.; Zhaomin, H.; Yue, W. J. A phosphorescent material with high and balanced carrier mobility for efficient OLEDs. *Chem Commun* **2011**, *47* (11), 3150-3152.

(19) Kang, S.; Lee, J. Y.; Kim, T. Unveiling the Root Cause of the Efficiency-Lifetime Trade-Off in Blue Fluorescent Organic Light-Emitting Diodes. *Electron Mater Lett* **2019**, DOI: 10.1007/s13391-019-00180-5.

- (20) Tabor, D. P.; Chiykowski, V. A.; Friederich, P.; Cao, Y.; Dvorak, D. J.; Berlinguette, C. P.; Aspuru-Guzik, A. Design rules for high mobility xanthene-based hole transport materials. *Chem Sci* **2019**, *10* (36), 8360-8366, DOI: 10.1039/c9sc01491h.
- (21) Yang, X.; Du, X.; Tao, S.; Huang, Y.; Ding, X.; Xue, R. Efficient hole-transporter for phosphorescent organic light emitting diodes with a simple molecular structure. *Org Electron* **2015**, *26*, 481-486, DOI: 10.1016/j.orgel.2015.08.011.
- (22) Shahnawaz; Sudheendran Swayamprabha, S.; Nagar, M. R.; Yadav, R. A. K.; Gull, S.; Dubey, D. K.; Jou, J.-H. Hole-transporting materials for organic light-emitting diodes: an overview. *J Mater Chem C* **2019**, *7* (24), 7144-7158, DOI: 10.1039/C9TC01712G.
- (23) Cias, P.; Slugovc, C.; Gescheidt, G. Hole transport in triphenylamine based OLED devices: from theoretical modeling to properties prediction. *J Phys Chem A* **2011**, *115* (50), 14519-25, DOI: 10.1021/jp207585j.
- (24) Fujikawa, H.; Ishii, M.; Tokito, S.; Taga, Y. J. M. P. Organic Light-Emitting Diodes Using Triphenylamine Based Hole Transporting Materials. *Mater. Res. Soc. Symp. Proc* **2000**, *621*, Q3.4.1.
- (25) Chen, R.; Bu, T.; Li, J.; Li, W.; Zhou, P.; Liu, X.; Ku, Z.; Zhong, J.; Peng, Y.; Huang, F. J. C. Efficient and Stable Inverted Planar Perovskite Solar Cells Using a Triphenylamine Hole - Transporting Material. *Chemsuschem* **2018**, DOI: 10.1002/cssc.201800476.
- (26) Chen, H.; Gao, C.-H.; Jiang, Z.-Q.; Zhang, L.; Cui, L.-S.; Ji, S.-J.; Liao, L.-S. Spiro-annulated hole-transport material outperforms NPB with higher mobility and stability in organic light-emitting diodes. *Dyes Pigments* **2014**, *107*, 15-20, DOI: 10.1016/j.dyepig.2014.03.006.

- (27) Wu, P.; Tian, G.; Hu, M.; Hong, L.; Dong, Q.; Liang, W.; Huang, J.; Su, J. J. T. Novel hole transport materials based on triarylamine/naphtho[2,1- *b*]benzofuran for efficient green electroluminescent device. *Tetrahedron* **2017**, *73* (31), 4610-4615.
- (28) Zheng, Z.; Dong, Q.; Gou, L.; Su, J.-H.; Huang, J. Novel hole transport materials based on N,N' -disubstituted-dihydrophenazine derivatives for electroluminescent diodes. *J. Mater. Chem. C* **2014**, *2* (46), 9858-9865, DOI: 10.1039/c4tc01965b.
- (29) Huang, X.-L.; Zou, J.-H.; Liu, J.-Z.; Jin, G.; Li, J.-B.; Yao, S.-L.; Peng, J.-B.; Cao, Y.; Zhu, X.-H. A high T_g small-molecule arylamine derivative as a doped hole-injection/transport material for stable organic light-emitting diodes. *Org Electron* **2018**, *58*, 139-144, DOI: 10.1016/j.orgel.2018.04.012.
- (30) Chen, S.; Jiang, S.; Yu, H. Diphenylamino-substituted bicarbazole derivative: Hole-transporting material with high glass-transition temperature, good electron and triplet exciton blocking capabilities and efficient hole injection. *Chem Phys Lett* **2017**, *674*, 109-114, DOI: 10.1016/j.cplett.2016.12.027.
- (31) Hreha, R. D.; George, C. P.; Haldi, A.; Domercq, B.; Malagoli, M.; Barlow, S.; Brédas, J. L.; Kippelen, B.; Marder, S. R. 2,7-Bis(diaryl amino)-9,9-dimethylfluorenes as Hole-Transport Materials for Organic Light-Emitting Diodes. *Adv Funct Mater* **2003**, *13* (12), 967-973, DOI: 10.1002/adfm.200304464.
- (32) Wu, P.; Tian, G.; Hu, M.; Lian, H.; Dong, Q.; Liang, W.; Huang, J.; Su, J. Novel hole transport materials based on triarylamine/naphtho[2,1- *b*]benzofuran for efficient green electroluminescent device. *Tetrahedron* **2017**, *73* (31), 4610-4615, DOI: 10.1016/j.tet.2017.06.031.

- (33) Braveenth, R.; Bae, H. W.; Nguyen, Q. P.; Ko, H. M.; Lee, C. H.; Kim, H. J.; Kwon, J. H.; Chai, K. Y. Spirobifluorene Core-Based Novel Hole Transporting Materials for Red Phosphorescence OLEDs. *Molecules* **2017**, *22* (3), DOI: 10.3390/molecules22030464.
- (34) Liao, Y.-L.; Hung, W.-Y.; Hou, T.-H.; Lin, C.-Y.; Wong, K.-T. Hole Mobilities of 2,7- and 2,2'-Disubstituted 9,9'-Spirobifluorene-Based Triaryldiamines and Their Application as Hole Transport Materials in OLEDs. *Chem Mater* **2007**, *19* (25), 6350-6357, DOI: 10.1021/cm702230e.
- (35) Chen, J.; Shi, W.; Jiang, Y.; Wang, D.; Shuai, Z. J. S. C. C. Strain induced polymorphism and band structure modulation in low-temperature 2,7-dioctyl[1]benzothieno[3,2-b][1]benzothiophene single crystal. *Sci China Chem* **2017**, *60* (2), 275.
- (36) Tong, S.; Jia, S.; Wang, C.; Huang, Y.; Zhang, C.; Shen, J.; Xie, H.; Niu, D.; Si, X.; Yuan, Y. High-Performance Broadband Perovskite Photodetectors Based on CH₃NH₃ PbI₃ /C₈BTBT Heterojunction. *Adv Electron Mater* **2017**, 1700058.
- (37) Jie, W.; Kan, Y. H.; Yong, W.; Su, Z. M. Computational Design of Host Materials Suitable for Green-(Deep) Blue Phosphors through Effectively Tuning the Triplet Energy While Maintaining the Ambipolar Property. *J Phys Chem C* **2013**, *117* (16), 8420–8428.
- (38) Ma, W.; Huang, J.; Li, C.; Jiang, Y.; Li, B.; Qi, T.; Zhu, X. One-pot synthesis and property study on thieno[3,2-*b*]furan compounds. *RSC Adv* **2019**, *9* (13), 7123-7127, DOI: 10.1039/c9ra00796b.
- (39) Wu, Y.; Li, W.; Jiang, L.; Zhang, L.; Lan, J.; You, J. Rhodium-catalyzed ortho-heteroarylation of phenols: directing group-enabled switching of the electronic bias for heteroaromatic coupling partner. *Chem Sci* **2018**, *9* (33), 6878-6882, DOI: 10.1039/c8sc02529k.

- (40) Chen, D.; Yuan, D.; Zhang, C.; Wu, H.; Zhang, J.; Li, B.; Zhu, X. Ullmann-Type Intramolecular C-O Reaction Toward Thieno[3,2-*b*]furan Derivatives with up to Six Fused Rings. *J Org Chem* **2017**, *82* (20), 10920-10927, DOI: 10.1021/acs.joc.7b01745.
- (41) Aaron, J.-J.; Párkányi, C.; Adenier, A.; Potin, C.; Zajíčková, Z.; Martínez, O. R.; Svoboda, J.; Pihera, P.; Váchal, P. Fluorescence Properties and Dipole Moments of Novel Fused Thienobenzofurans. Solvent and Structural Effects. *J Fluoresc* **2011**, *21* (6), 2133, DOI: 10.1007/s10895-011-0914-3.
- (42) Aitken R. A.; Bradbuty C. K.; Burns G.; Morrison J. J. Tandem Radical Cyclisation in the Flash Vacuum Pyrolysis of 2-Methoxyphenyl and 2-Methylthiophenyl Substituted Phosphorus Ylides. *Synlett* **1995**, *1995*(1), 53-54.
- (43) Fang, D. Q.; Sun, Y.; Chen, Y. Q.; Fu, T. C.; Ali, M. U.; He, Y. W.; Miao, J. S.; Yan, C. Y.; Meng, H. Dibenzofuran-based iridium complexes as green emitters: Realizing PhOLEDs with high power efficiency and extremely low efficiency roll-off. *Dyes Pigments*, **2020**, *173*, 107990.
- (44) Kondrasenko, I.; Tsai, Z. H.; Chung, K. Y.; Chen, Y. T.; Ershova, Y. Y.; Domenech-Carbo, A.; Hung, W. Y.; Chou, P. T.; Karttunen, A. J.; Koshevoy, I. O. Ambipolar Phosphine Derivatives to Attain True Blue OLEDs with 6.5% EQE. *ACS Appl Mater Interfaces* **2016**, *8* (17), 10968-76, DOI: 10.1021/acsami.6b01041.
- (45) Cao, C.; Chen, W. C.; Chen, J. X.; Yang, L.; Wang, X. Z.; Yang, H.; Huang, B.; Zhu, Z. L.; Tong, Q. X.; Lee, C. S. Bipolar Blue Host Emitter with Unity Quantum Yield Allows Full Exciton Radiation in Single-Emissive-Layer Hybrid White Organic Light-Emitting Diodes. *ACS Appl Mater Interfaces* **2019**, *11* (12), 11691-11698, DOI: 10.1021/acsami.9b01105.

Journal Pre-proof

Highlights

1. We developed a strategy to design high efficient HTM for RGB OLEDs and explored a new way to synthesize **BTBF** moiety efficiently, which is the first time to be utilized in OLEDs.
2. For Green PhOLEDs, the maximum current efficiency (CE) of 123.6 cd A^{-1} , power efficiency (PE) of 136.6 lm W^{-1} , and external quantum efficiency (EQE) of 34.1%. Red PhOLEDs exhibited a CE of 32.3 cd A^{-1} , PE of 40.1 lm W^{-1} , and EQE of 24.9% with a low turn on voltage of 2.3 eV. Blue fluorescence OLEDs presented a maximum CE of 4.7 cd A^{-1} , PE of 4.9 lm W^{-1} , and EQE of 5.2% with small efficiency roll-off of 11.5% at 10000 cd m^{-2} .
3. Furthermore, we tested device lifetime of **BTBF-DPA** based RGB OLEDs, which are $T_{99} = 70 \text{ h}$ at 10000 cd m^{-2} , $T_{70} = 60 \text{ h}$ at 10000 cd m^{-2} , $T_{80} = 125 \text{ h}$ at 5000 cd m^{-2} , respectively.

Declaration of interests

The authors declare that they have no known competing financial interests or personal relationships that could have appeared to influence the work reported in this paper.

The authors declare the following financial interests/personal relationships which may be considered as potential competing interests:

Journal Pre-proof